ELSEVIER

Biophysical Chemistry 110 (2004) 191–201

Biophysical Chemistry

www.elsevier.com/locate/bpc

The role of Zn in the interplay among Langmuir–Blodgett multilayer and myelin basic protein: a quantitative analysis of XANES spectra

M. Benfatto[a], S. Della Longa[b], Y. Qin[c], Q. Li[c], G. Pan[c], Z. Wu[d], S. Morante[e,*]

[a] *Laboratori Nazionali di Frascati LNF-INFN, Frascati, Italy*
[b] *University of L'Aquila, L'Aquila, Italy, and LNF-INFN, Frascati, Italy*
[c] *State Key Laboratory of Environmental Aque, Research Center for Eco-Environmental Sciences, Chinese Academy of Sciences, Beijing 100085, China*
[d] *Beijing Synchrotron Radiation Facility Institute of High Energy Physics, Chinese Academy of Sciences, P.O. Box 918, Beijing 100039, China*
[e] *Department of Physics, University of Rome "Tor Vergata", Via della Ricerca Scientifica 1-00133, Roma, Italy*

Received 9 February 2004; received in revised form 9 February 2004; accepted 13 February 2004
Available online 9 April 2004

Abstract

We have performed a quantitative analysis of the X-ray absorption near-edge structure (XANES) spectra at the Zinc K-edge of systems formed by phospholipid Langmuir–Blodgett multilayers (LBMLs) in the presence and in the absence of myelin basic protein (MBP) and in two hydration conditions. These spectra have been analysed by a new procedure called Minuit XANes (MXAN) which is able to perform a quantitative fit of XANES data in terms of structural parameters. By this method, we have been able to correlate the relevant differences between the spectra observed in the XANES range with the coordination changes due to reduction of the space around the Zinc when the level of hydration is lowered and/or the myelin basic protein is added. These spectral differences are peculiar of the XANES energy range, and are not present in the extended X-ray absorption fine structure (EXAFS) energy range where the analysis was previously performed. With this investigation, we give an unambiguous answer to the question of the role of zinc in such complexes by showing that the metal interacts with both the phospholipid heads of the substrate and the myelin basic protein.

Keywords: Langmuir–Blodgett multilayers; Myelin basic protein; Zinc; X-ray absorption spectroscopy; Near-edge structure

1. Introduction

The myelin sheath is a rather unique multilamellar membrane formed by many lipid bilayers tightly wrapped around the nerve axon. Its integrity is crucial for the efficiency of the signal transduction along the axon. The myelin basic protein (MBP) is known to play a crucial role in ensuring the stability of the myelin sheath [6,27]. The efficiency of MBP in preserving the compactness and the stability of the myelin membrane appears to be enhanced in the presence of zinc (Zn) ions [4,12]. There are also

* Corresponding author. Tel.: +39-672594554; fax: +39-62025259.
E-mail address: morante@roma2.infn.it (S. Morante).

0301-4622/$ - see front matter © 2004 Elsevier B.V. All rights reserved.
doi:10.1016/j.bpc.2004.02.003

evidences [8] that Zn stabilizes the "in vitro" self-association of MBP dissolved in a phosphate buffer.

In order to understand the role played by Zn in these aggregates one must get, as a necessary first step, a precise information on the nature of the interaction of Zn ions with myelin sheath components.

The multilamellar structure of the myelin sheath is quite accurately modeled by Langmuir–Blodgett multilayers (LBMLs). Indeed, these model membranes have been extensively used to obtain quantitative information on the molecular organization between phospholipid and MBP molecules with the help of a number of complementary experimental techniques [16].

X-ray absorption spectroscopy (XAS) has been recently employed to investigate the local environment of Zn ions inserted in LBMLs. These studies have suggested [21,25] that the geometry around the metal is significantly different from that of Zn in water. Furthermore, a qualitative analysis of the X-ray Absorption Near Edge Structure (XANES) region of the spectrum has shown a correlation between on the one hand the appearance of a peculiar preedge structure in the spectrum and on the other the presence of MBP and the level of hydration in the region between the heads of two adjacent phospholipid layers.

However, because the extended X-ray absorption fine structure (EXAFS) high-energy region appeared unaffected by such physical and chemical modifications, the previous authors were led to the conclusion that the examined samples were characterized by an almost identical short range atomic arrangement around the Zn, thus excluding that the differences found in the XANES part of the spectrum were to be attributed to differences in the coordination number or the chemical nature of nearby scatterers.

With the purpose of extracting useful information from the appearance of this peculiar preedge structure in the measured XAS spectra, in this paper we reconsider and analyse in a detailed way the whole XANES region.

The analysis of the XANES region turns out to be of great interest for structural studies of biological systems. In fact, despite the fact that the magnitude of the scattering amplitudes from light elements (which biological systems are mostly made of) severely limits the energy range of the available experimental data, the precise form of the spectrum in the low-energy region is extremely sensitive to a variety of structural details that are often crucial for our understanding of the subtle relations between structure and function. Consequently, useful comparative information about the Zn coordination mode in different samples can be obtained, also in situations, like the biological ones, in which the physicochemical conditions of the systems under study are only marginally different. In this context, a paradigmatic example, in which a lot of work has been done with remarkable success, is given by the many XAS studies of the stereochemistry and functional properties of the active site in metallo-proteins, carried out in recent years (Ref. [17] and references therein).

As for our ability in extracting useful information from the data, it should be observed that today there exist several packages based on an accurate analysis of multiple scattering (MS) events capable of adequately reproducing the EXAFS spectroscopic signal (for a review, see Ref. [26]). On the contrary, the potentialities offered by the analysis of the near-edge region have not been yet fully exploited and the information encoded in the structure of the XANES spectrum have been until very recently exploited only at a qualitative level.

This situation has markedly changed with the introduction of a new approach [2], implemented in a code called Minuit XANes (MXAN), capable of yielding a quantitative analysis of the region from the edge up to 200 eV above threshold. The method takes into account MS events in a rigorous way through the evaluation of the scattering wave operator [24]. The effectiveness of this approach has been already successfully tested in a number of interesting situations [3,9–11].

In this paper, we employ the MXAN strategy to extract local structural information around the Zn site in phospholipid LBMLs in the absence and in the presence of MBP molecules and in two different hydration conditions. The measured Zn K-edge XANES are quantitatively analysed and the results compared with those obtained by performing the same analysis on two model systems. The parameters that define the geometry are obtained by fitting the experimental data to the phenomenological model implemented in the MXAN package.

One finds in this way that the average coordination geometry around the Zn ions is essentially tetrahedral

in the maximal hydration condition in the absence of MBP, but it "flattens" down in the minimal hydration condition in the presence of the protein.

2. Materials and methods

2.1. Model compounds

A model sample where the scatterers around Zn are known to assume a tetrahedral geometry has been prepared by the following adsorption procedure.

An adsorption isotherm under specific adsorbent condition was produced by preparing a series of solutions with different initial concentrations of the metal (Zn in our case) in a number of centrifuge tubes with each tube containing the same concentration of manganite (γ-MnOOH) as adsorption support.

Manganite was prepared according to Giovanoli and Leuenberger [15]. Mn(II), which is present as $MnSO_4$, is oxidized with 30% H_2O_2 and forced to precipitation by adding 0.2 M of NH_3. The surface area of manganite, measured by the Brunauer–Emmet–Teller (BET) method [7], was 57.64 m^2/g.

Hydrous manganese oxide (δ-MnO_2) was prepared by slowly adding Mn(II) nitrate, potassium permanganate, and sodium hydroxide in the mole ratio 3:2:4. Before using it in adsorption studies, δ-MnO_2 was filtered, washed and redispersed in distilled water, its pH was adjusted to be around 6, and it was aged for 16–20 h.

Adsorption experiments were then performed at constant ionic strength and temperature (25.0±0.1 °C). After 24 h of equilibration, every sample was removed by centrifugation and the concentration of the metal (Zn^{2+}) dissolved in the aqueous phase was determined by Anodic Stripping Voltmeter (ASV) measurements. The concentration of the Zn^{2+} ions adsorbed or surface bound to particles or colloids was then established by difference method, not being accessible to ASV measurements. The resulting wet paste was mounted in a 2-mm-thick cell and sealed for EXAFS experiments.

The Zn K-edge XANES spectra of the tetrahedral model compound obtained in this way were measured in fluorescence mode with a Si (111) double crystal monochromator at the beam line 4W1B of the Beijing Synchrotron Radiation Facility (BSRF). The storage ring was working at the typical energy of 2.2 GeV with an electron current of about 100 mA. Spectra were recorded in the energy range 9.6–9.9 keV with an energy resolution of 1.5 eV. Standard background subtraction procedure was employed in data reduction.

The Zn^{2+} in water solution, taken as model for octahedral geometry, has been prepared according the method presented in D'Angelo et al. [9].

2.2. Biological samples

L-alpha-Dilauroylphosphatidic acid LBML's from a subphase of a 10^{-3} M solution of $ZnCl_2$, in the presence and in the absence of MBP were subjected to XAS measurements, as described in Morante [21] and Nuzzo et al. [25]. XAS spectra were collected at the Italian beamline BM8-GILDA of the European Synchrotron Radiation Facility (ESRF) in Grenoble. Spectra were acquired in fluorescence mode at the Zn K-edge, achieving an energy resolution of about 0.4 eV. The following four types of samples were measured:

- LBMLs in the absence of MBP, in air (from now on s_a for short);
- LBMLs in the absence of MBP, in vacuum (s_b);
- LBMLs in the presence of MBP, in air (s_c);
- LBMLs in the presence of MBP, in vacuum (s_d).

3. Data analysis

For the purpose of extracting information on the structural arrangement of atoms around Zn ions and its dependence on the physicochemical nature of the Zn environment, we have decided to reanalyse the XANES data of the samples s_a and s_d, because we expect their geometries to show the most pronounced difference. They, in fact, correspond to complexes where Zn ions experience the more different physicochemical conditions. In the present work, we present a new analysis of the XANES region of the spectra of samples s_a and s_d, employing the theoretical framework implemented in the MXAN code.

The main novelty of the theoretical approach implemented in MXAN lies in the fact that it provides the "exact" solution of the photoelectron Schrödinger problem by directly computing the inverse of the complete wave operator [24], instead of expanding

the solution in powers of the free Green function, as is done, e.g., in the gnXAS analysis code [1,13,14]. In this way, all the MS contributions are automatically taken into account and the absorption coefficient is directly given as a function of the energy. This last feature allows an immediate comparison of theory with experimental data with no need to go to the k space.

MXAN has a simple modular structure and incorporates related codes developed by Natoli and Benfatto [24] and Tyson et al. [28] in the last years that, among other features, allows to include hydrogen atoms in the calculation.

The fitting procedure is based on a first comparison of the experimental data to the results of a large number (of the order of hundred) of different theoretical calculations performed starting from different model geometrical arrangements of scatterers around the absorber. Such models are obtained by randomly varying selected structural parameters. The final refinement in parameter space is carried out employing standard minimization routines, like MINUIT, a freely available package of the CERN computing library [18], to minimize the square residual function

$$\chi^2 = \frac{1}{m-n}\sum_{i=1}^{m}\frac{(y_i^{\mathrm{th}} - y_i^{\mathrm{ex}})^2}{\varepsilon_i^2} \quad (1)$$

where n is the number of independent parameters let to vary in the fit, m is the number of experimental data, y_i^{th} and y_i^{ex} are the theoretically computed and experimentally measured values of the absorption coefficient, respectively, and ε_i is our estimate of the experimental error, that is kept constant during the fitting.

Inelastic losses are taken into account by convoluting the computed signal with a broadening Lorentzian function having an energy dependent width of the form

$$\Gamma(E) = \Gamma_{\mathrm{c}} + \Gamma_{\mathrm{mfp}}(E) \quad (2)$$

The constant part Γ_{c} accounts for the core-hole life time, as well as for the experimental resolution, while the energy-dependent term $\Gamma_{\mathrm{mfp}}(E)$ [22] represents all the inelastic processes that in the EXAFS analysis are included in the term which depends on the electron mean free path (mfp). Both terms are refined during the fitting procedure at each step of the computation, on the basis of a Monte Carlo search in the parameter space, in a way similar to the procedure used in optimisation by simulated annealing [20]. Muffin-Tin (MT) radii of the external potential are chosen according to D'Angelo et al. [9]. In the following figures, the XANES spectra are presented in arbitrary units with the absorption jump at the edge normalised to unity. In Eq. (1), a conservative error ε equal to 0.018 units (1.8% of the absorption jump) has been attributed to all data points ($\varepsilon=\varepsilon_i$). With this choice, the statistical error evaluated by the MIGRAD routine of the MINUIT package for the parameters is never worse than 3–5%.

4. Results

In Fig. 1, the Zn K-edge XANES spectra of the four samples s_a, s_b, s_c and s_d (from top to bottom) are reported. In the high-energy region, where the stan-

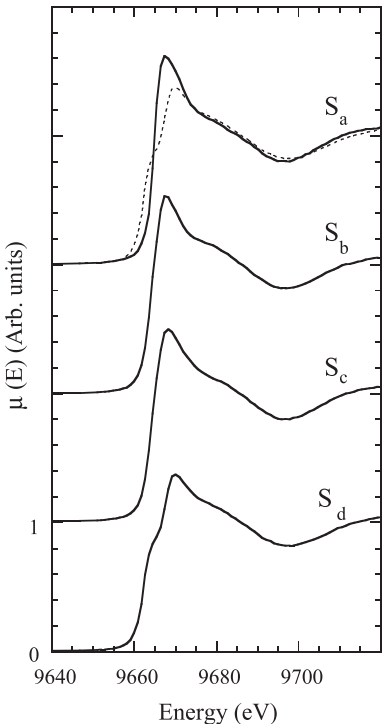

Fig. 1. Zn K-edge XANES spectra of LBML samples. From top to bottom: s_a in the absence of MBP, in air; s_b in the absence of MBP, in vacuum; s_c in the presence of MBP, in air; s_d in the presence of MBP, in vacuum. The spectrum of sample s_d is also shown superimposed (dotted line) to that of s_a for comparison.

dard EXAFS analysis can be reliably employed [25], the four spectra are all very similar, whereas relevant differences appear around the edge. In same figure, the spectrum s_d is also drawn superimposed (dotted line) to the spectrum of s_a, to more clearly exhibit their differences. While the s_a spectrum shows a single peak at about 9667 eV, the s_d spectrum shows, besides a lower peak at 9670 eV, a pronounced shoulder around 9665 eV. As will be discussed in more detail below, the appearance of edge structures, like the shoulder observed in s_d, is in general interpreted as the symptom of a lowering of the degree of symmetry in the geometrical arrangement of the scattering atoms around the absorber [24].

The analysis of the EXAFS region of the spectra of the four s_i samples, done by Morante [21] and Nuzzo et al. [25], has proved that in all cases Zn is tetra-coordinated. The four ligands are light atoms, possibly oxygen, at a mean distance of about 1.96 Å. They may belong to water molecules or to the phosphate groups of the phospholipid heads, or else, in the case of the samples where MBP is present (samples s_c and s_d), also to protein residues. Moreover, the analysis of whole set of experimental data confirms that the Zn coordination is markedly different from the hexa-coordinated, regular octahedral arrangement of Zn in water.

A parameter that to some extent affects the form of the spectrum is the hydration level of the lipid multilayer. This is seen (Fig. 2) by comparing among themselves the XANES difference spectra s_b-s_d (solid line), s_a-s_b (dotted line), s_a-s_d (dashed line) and s_a-s_c (dotted-dashed line). From their comparison, one first of all notices that the geometrical distortion induced by a modification of the hydration level (s_a-s_b) and that induced by the presence of the protein at the highest hydration level (s_a-s_c) are not really experimentally distinguishable. In particular, while the height of the preedge shoulder at 9663 eV increases, the height of the peak at about 9667 eV decreases both by lowering the hydration level as well as by adding the protein. Furthermore, height variation is maximal when simultaneously the hydration level is lowered and the protein is added (s_a-s_d). On the other hand, the two spectra s_b and s_d (samples with and without the protein, respectively, at the lowest hydration level) show significant differences (see the s_b-s_d spectrum), which essentially account for almost the whole difference between the two extreme situations s_a and s_d.

All these results taken together indicate that more than one single geometrical configuration of scatterers around the Zn site must be present and contributes to the structure of the XANES spectra. It must be, however, remarked that the possible different local

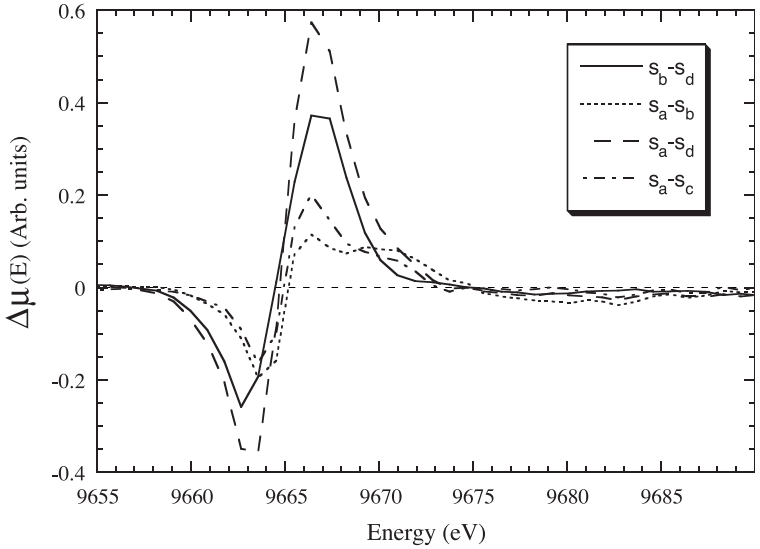

Fig. 2. XANES difference spectra s_b-s_d (solid line), s_a-s_b (dotted line), s_a-s_d (dashed line) and s_a-s_c (dotted-dashed line).

atomic arrangements should all be compatible with the fourfold coordination mode that unmistakably results from the EXAFS analysis of Morante [21] and Nuzzo et al. [25]. Possible geometries range with continuity between purely (i.e., undistorted) tetrahedral and square-planar arrangements.

Taking into account these constraints, we have attempted a quantitative analysis of the XANES spectra of the two samples s_a (i.e., LBMLs in air in the absence of MBP) and s_d (i.e., LBMLs at the lowest level of hydration in the presence of MBP), because, as we said above, they represent the two most distant physicochemical situations for which we have experimental data.

Our procedure will be to start by first examining the MXAN analysis of the XANES spectra of two model systems, Zn in bulk water and Zn adsorbed at the water–manganite interface. While Zn in water is known to be octahedrically coordinated [9], the Zn adsorbed at the water–manganite interface is found to be tetra-coordinated [5] and it is possibly representative of the situation experienced by Zn in LBMLs. The good quality of the fits one gets is a test of the ability of MXAN to correctly interpret the experimental data. Armed with this knowledge, we have proceeded to determine the (average) geometry around the Zn ions in the physically interesting case of the s_a and s_d systems, trying different geometries starting with the planar square one.

4.1. MXAN analysis of model systems

Fig. 3 shows the XANES part of the spectrum of Zn^{2+} in aqueous solution (upper curve, a, ○). The XAS spectrum of this system [9] is taken as a model of regular octahedral coordination for the metal. The analysis of the EXAFS data yields an average Zn–O distance $r=2.08\pm0.04$ Å.

The measured XANES spectrum of Zn adsorbed at the water–manganite interface is also shown in Fig. 3 (lower curve, b, ○). The analysis of the EXAFS region performed by Bochatay and Persson [5] shows a first coordination shell with an average Zn–O distance $r=1.95\pm0.04$ Å.

We now discuss the theoretical calculations of the XANES region of the spectra according to the approach of Benfatto and Della Longa [2] implemented in the MXAN code.

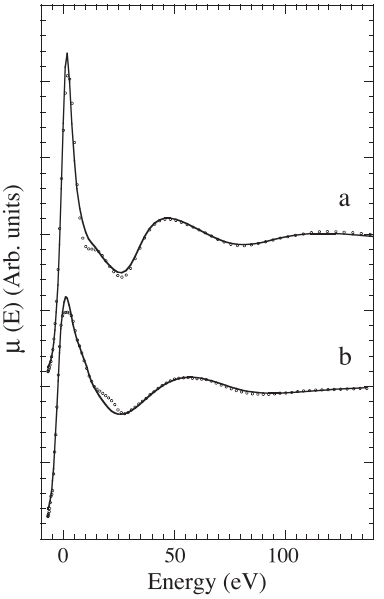

Fig. 3. (a) Experimental XANES spectrum of Zn^{2+} in aqueous solution (○) superimposed to the MXAN best fit spectrum (solid curve) corresponding to a regular octahedral symmetry with six oxygens at a distance $r=2.08\pm0.04$ Å from Zn. (b) Experimental XANES spectrum of Zn adsorbed at the water–manganite interface superimposed to the MXAN best fit spectrum (solid curve) corresponding to a pseudotetrahedral coordination geometry with four oxygens at a distance $r=1.98\pm0.04$ Å and flattening angle $\alpha_1=\alpha_2=120°\pm6°$ (see Fig. 4).

The XANES analysis of Zn^{2+} ion in aqueous solution has been reported in detail in D'Angelo et al. [9]. By using a single parameter to fit the spectrum, a value of the Zn–O distance $r=2.06\pm0.02$ Å with a $\chi^2=2.85$ ($n=1$) is obtained, in good agreement with the EXAFS result. The theoretical spectrum is drawn in Fig. 3 (solid lines, a, upper curve) superimposed to the experimental data.

We performed a fit of the XANES spectrum of Zn in manganite by varying the Zn–O distance and the so-called flattening angles, α_i, $i=1, 2$ (see Fig. 4). The flattening angles α_i are kept equal in the fit and varied in the range between 109° (a configuration corresponding to a regular tetrahedral geometry) and 180° (a configuration corresponding to a square planar geometry). The best fit gives a value $r=1.98\pm0.06$ Å for the Zn–O distance and flattening angles $\alpha_1=\alpha_2=120\pm6°$, leading to a fairly good $\chi^2=2.69$ ($n=2$).

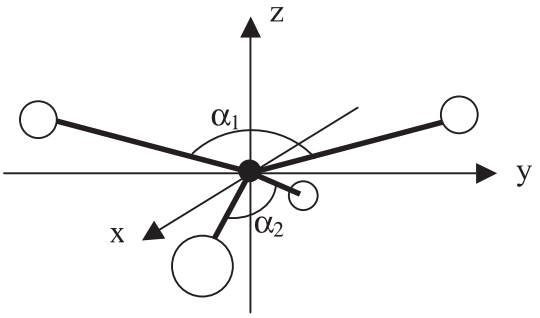

Fig. 4. Scatterers arrangement around the Zn ion defining the flattening angles α_1 and α_2.

This analysis shows that the MXAN approach, besides confirming the results obtained from the analysis of the EXAFS region, is capable of giving rather accurate information about the arrangement of the scatterers around the metal. The small differences in the height of the main peak between the theoretical curve and the experimental data and the minor discrepancies around 15–20 eV that one sees in both fits (Fig. 3) are most probably due to the somewhat inadequate MT approximation employed to model the form of the external potential [2,19].

4.2. MXAN analysis of the LBLM samples

We now discuss the fit to the XANES part of the spectrum of the samples s_a and s_d. The starting models for the geometrical arrangements of atoms around the Zn were constructed taking into account the results obtained in Morante [21] and Nuzzo et al. [25]. Because the EXAFS results clearly indicate that in both cases Zn is tetra-coordinated, the fitting MXAN procedure starts assuming the existence of four water molecules sitting around the Zn site, in a planar geometrical arrangement (flattening angles are assigned the initial values $\alpha_1=\alpha_2=180°$, see Fig. 4). To avoid biasing the fit too much towards the EXAFS results, the four water oxygens were located at distances, r_i, from the Zn absorber fairly different from those obtained from the EXAFS fit. For the sample s_a we decided to take $r_1=r_2=r_3=r_4=2.08$ Å, compared to the average value1.96 Å of Nuzzo et al. [25]. Contributions from hydrogen atoms were explicitly included. In Fig. 5, the experimental spectrum (○) and the best fit result (solid line) are shown. The fit reproduces rather well the main features of the experimental spectrum, giving $\chi^2=1.58$ with $n=6$ (the four distances, r_i, and the two angles of Fig. 4). The best fit

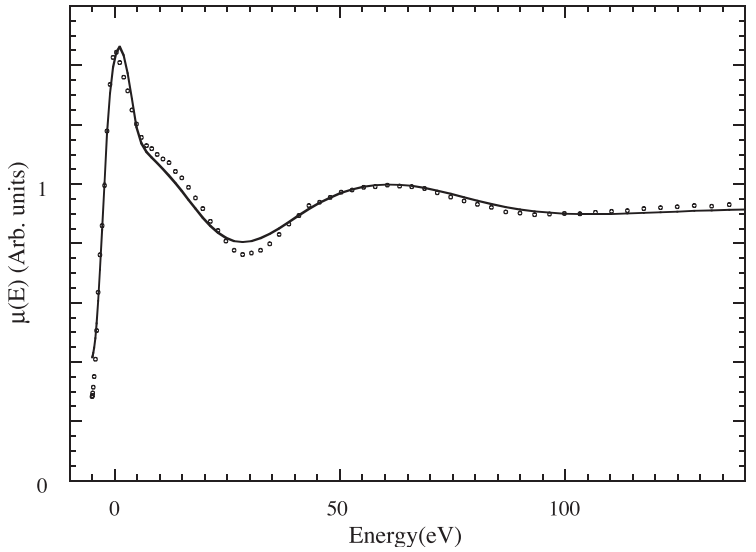

Fig. 5. Experimental Zn K-edge XANES spectra of LBMLs in the absence of MBP (○) in air (s_a); theoretical MXAN spectrum (solid curve) corresponding to the best fit structure (four ligands, six parameters) with flattened tetrahedral coordination geometry and Zn–O distances $r_1=1.89\pm0.04$ Å, $r_2=1.84\pm0.04$ Å, $r_3=1.99\pm0.04$ Å, $r_4=1.99\pm0.04$ Å and flattening angles $\alpha_1=124°\pm6°$, $\alpha_2=106°\pm6°$.

values are r_1=1.89±0.05 Å, r_2=1.84±0.05 Å, r_3=1.99±0.06 Å, r_4=1.99±0.06 Å, α_1= 124±6° and α_2=106±5°, corresponding to an almost tetrahedral coordination of four water molecules around the Zn ion. These findings are in good agreement with previous EXAFS results [25] and add to them new information about the flattening angles. Recalling that the Zn in manganite is tetrahedrically coordinated, the overall geometrical picture we obtain is also well in line with the observed overall similarity between the two experimental spectra (s_a and Zn in manganite).

Attempts to fit the spectrum of the s_d sample with the same geometry as s_a, is unsatisfactory. The s_d spectrum is also quite different from that of Zn in aqueous solution, where scatterers are arranged in a regular octahedral geometry. In particular, neither with a distorted tetrahedral nor a regular octahedral geometry, it is possible to satisfactorily reproduce the characteristic edge shoulder at about 9665 eV (Fig. 1). As a general remark, we recall that the presence of a shoulder in the rising edge of a XANES spectrum indicates an asymmetrical coordination geometry with large distortions of nearest neighbour scatterer distances [23,28]. For this reason, a sixfold, pseudooctahedral geometry having large orthorhombic distortion was assumed in fitting the s_d spectrum, with the two axial atoms located at a much larger distance from the metallic site than the four equatorial oxygens.

Two different fits were tried, according to whether the equatorial oxygens are taken with or without bound hydrogens. The corresponding theoretical spectra will be called $\mu^d{}_H$ and $\mu^d{}_{noH}$, respectively. The experimental spectrum of the s_d sample (○) and the calculated spectra corresponding to the best fit results are reported in Fig. 6 ($\mu^d{}_H$ spectrum) and Fig. 7 ($\mu^d{}_{noH}$ spectrum).

The fit with bound hydrogens (Fig. 6) gives χ^2=2.53, with n=6 (four distances and two angles). We only let four distances to vary by imposing the constraints $r_1=r_2$ and $r_3=r_4$ in the plane, while letting the long axial distances, r_5 and r_6, to vary independently. Besides, α_1 and α_2 are kept as independent parameters. The best fit values are $r_1=r_2$=1.81±0.04 Å, $r_3=r_4$=2.03±0.06 Å, r_5=2.74±0.07 Å, r_6=2.96±0.07 Å, α_1= 176°±6° and α_2=154°±6°.

The fit with no bound hydrogens (Fig. 7) yields a value χ^2=2.22 (again n=6) with the following best fits values $r_1=r_2$=1.94±0.05 Å, $r_3=r_4$=1.94±0.05 Å, r_5=2.77±0.07 Å, r_6=2.82±0.07 Å, α_1= 170°±6° and α_2=176°±6°.

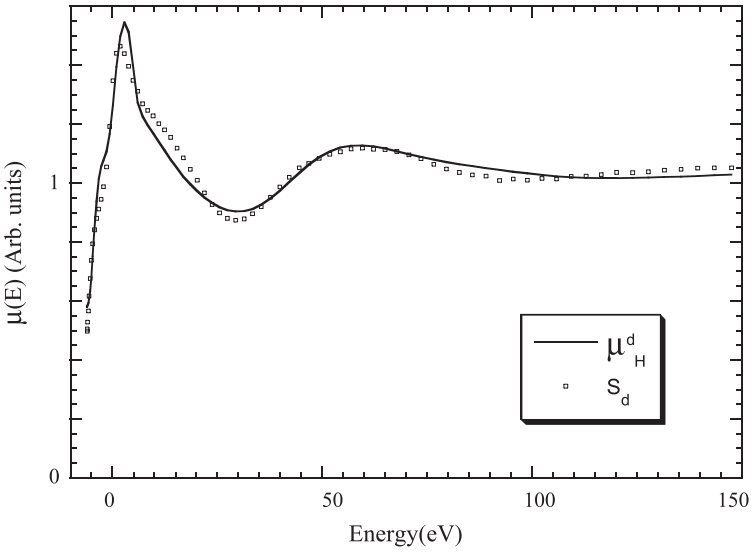

Fig. 6. Experimental XANES spectrum (○) LMBL in the presence of MBP, in vacuum (s_d); theoretical MXAN spectrum including water-bound hydrogens (solid curve) corresponding to the best fit structure (six ligands, six parameters) with flattened tetrahedral coordination geometry and Zn–O distances $r_1=r_2$=1.81±0.04 Å, $r_3=r_4$=2.03±0.04 Å, r_5=2.74±0.07 Å, r_6=2.96±0.07 Å, and flattening angles equal to α_1= 176°±6°and α_2=154°±6°.

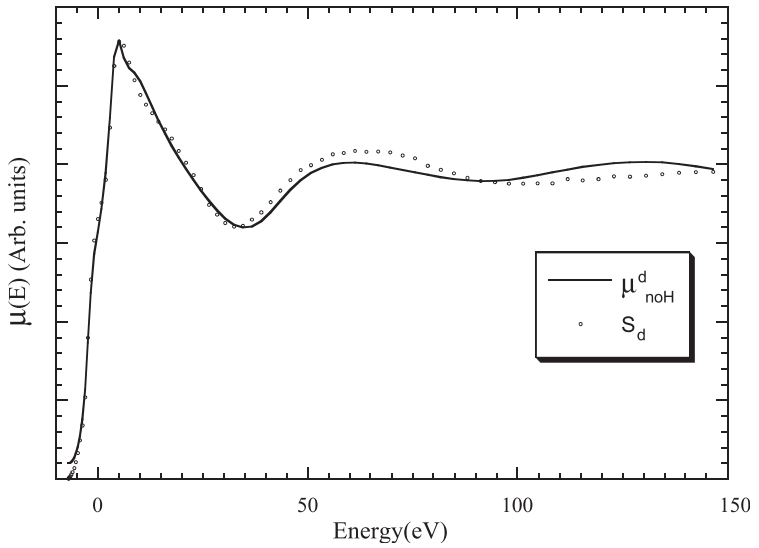

Fig. 7. Experimental XANES spectrum (○) LMBL in the presence of MBP, in vacuum (s_d); theoretical XANES spectrum without hydrogens (solid curve) corresponding to the best fit structure (six ligands, six parameters) with flattened tetrahedral coordination geometry and Zn–O distances r_1=r_2=1.94±0.04 Å, r_3=r_4=1.94±0.04 Å, r_5=2.77±0.07 Å, and r_6=2.82±0.07 Å and flattening angles α_1= 170°±6° and α_2=176°±6°.

The second model is characterized by a better χ^2 and reproduces more accurately the relevant features of the experimental spectrum, especially the rise of the edge shoulder and the shape of the bump around threshold. However, in many details the experimental data and the theoretical curve differ for energies above threshold. For these reasons, numerous other fits have been attempted with different numbers of free parameters and different types of axial ligands (for example, phosphate groups instead of the axial oxygens have

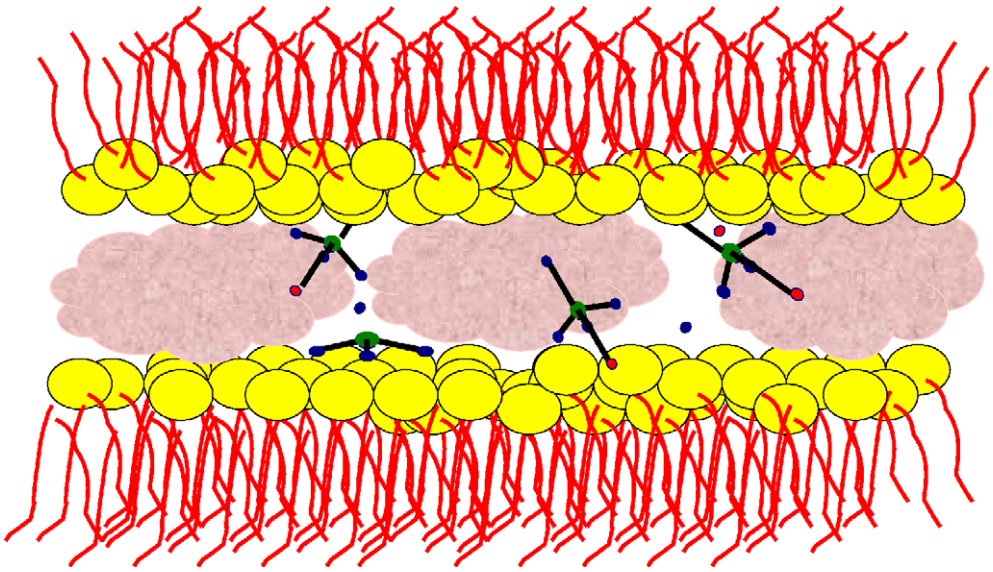

Fig. 8. Pictorial view of the Zn environment in LMBLs in the presence of MBP in vacuum, according to our results. The majority of the Zn ions adsorbed on the surface of the lipid heads is also bound to the protein. Some of them remain embedded within nearby phospholipid heads.

been included to mimic the interaction of Zn ions with the phosphatidic heads). In all the cases, we have tried the fit leads to a geometrical arrangement which always requires a more or less distorted equatorial plane formed by four oxygens at a distance of about 1.95 Å from the Zn, plus two axial ligands with distances ranging between 2.5 and 3.0 Å, depending on the details of the chosen model geometry.

None of these attempts led to a significant improvement of the overall quality of the fit, although with an appropriate "tuning" of the model, separated portions of the energy interval could be fitted with high accuracy. The situation suggests that multiple configurations of the Zn coordination geometry are simultaneously present in the measured samples. This interpretation is in line with a model of the interactions of the Zn ion in LBMLs in the presence of MBP in which a high fraction of ions is adsorbed between the protein and the phopholipids heads of LBMLs, while a smaller fraction is adsorbed within nearby phopholipids heads (Fig. 8). A nice confirmation of this model comes from the observation that, as shown in Figs. 6 and 7, the overall quality of the fit of sample s_d is higher if the contribution from oxygen bound hydrogen atoms is removed (μ^d_{noH} spectrum), despite the fact that the high energy region is more accurately fitted if hydrogens are included (μ^d_H spectrum). This peculiar situation can be explained assuming that a fraction of Zn ions is always bound to four water molecules and thus retains the same geometrical configuration as in the sample s_a.

5. Conclusions

Recent XAS experiments [21,25] have proved that, when LBMLs are grown in the presence of Zn ions, the metal remains trapped in between two adjacent LB layers. The analysis of the recorded EXAFS spectra, formerly carried out by these authors, showed that the coordination mode of the Zn in all the measured samples (i.e., in the presence or in the absence of MBP and at two different hydration levels) is definitely different from that of Zn in water. Qualitative considerations based on general features of the XANES part of the spectrum suggested some sort of interaction between Zn ions and the lipid heads of the phospholipid molecules.

In this paper, we have subjected to an accurate quantitative analysis the edge region of the XAS spectrum of Zn adsorbed at the water–manganite surface (Fig. 3b), as well as the spectra of Zn immersed in LBMLs in two situations, namely in the absence of MBP and at the highest explored hydration level (sample s_a, Fig. 5) and, at the other extreme, in the presence of MBP and at low hydration level (sample s_d, Figs. 6 and 7).

We find that the structural parameters emerging from the MXAN fitting algorithm of the spectrum of Zn ions adsorbed at the water–manganite interface and those emerging from the fit to the s_a sample are very indicative of highly similar geometric arrangement of scatterers around the metal. In both cases, the geometry around the Zn turns out to be that of a slightly distorted tetrahedron, definitely different from the fully symmetrical octahedral geometry of Zn in water (Fig. 3a). The similarity of the atomic arrangement that we find should be taken as a strong indication of the fact that also in this last case Zn finds itself in a constrained environment rather similar to that experienced at the water–manganite interface. We conclude that in the s_a sample, there must be a direct interaction of Zn ions laying within two adjacent LB layers with the "surface" of the lipid heads.

The quantitative analysis of the XANES region of sample s_d confirms this picture, showing that multiple configurations of Zn coordination geometries are simultaneously present. A large fraction of ions adsorbed between the protein and the phopholipids heads of LBMLs are responsible for the appearance of some new features in the spectrum, like the enhancement of the preedge shoulder. At the same time, there is a small fraction of Zn ions that is still located within two adjacent of phospholipid heads. The coordination mode of the latter is rather similar to that of Zn ions at the water–manganite interface and in the sample s_a.

We would like to conclude by saying that a quantitative XANES analysis requires quite a sophisticated discussion of the geometry of the metallic site. We have nevertheless been able to obtain a satisfactory and more complete picture of the Zn environment in the various physicochemical situations we have studied, thus enlightening the role played by the Zn in stabilizing the interaction between LMBL and MBP.

Acknowledgements

We thank G.C. Rossi for a careful reading of the manuscript. Discussions with C. Meneghini are acknowledged. We also thank P. D'Angelo for kindly giving us the experimental data of Zn^{2+} in water. Partial financial support from INFM, Italy, is gratefully acknowledged.

References

[1] M. Benfatto, C.R. Natoli, A. Bianconi, J. Garcia, A. Marcelli, M. Fanfoni, I. Davoli, Multiple-scattering regime and higher-order correlations in X-ray-absorption spectra of liquid solutions, Phys. Rev., B Condens. Matter 34 (8) (1986) 5774–5781.

[2] M. Benfatto, S. Della Longa, Geometrical fitting of experimental XANES spectra by a full multiple-scattering procedure, J. Synchrotron Radiat. 8 (2001) 1087–1094.

[3] M. Benfatto, P. D'Angelo, S. Della Longa, N.V. Pavel, Evidence of distorted fivefold coordination of the Cu^{2+} aqua ion from an X-ray absorption spectroscopy quantitative analysis, Phys. Rev., B 65 (174205-1/5).

[4] H.H. Berlet, H. Ilzenhofer, M. Noue, Metal cations and binding of extrinsic protein of bovine myelin, Biol. Chem. Hoppe-Seyler 378 (1987) 1246.

[5] L. Bochatay, P. Persson, Metal ion coordination at the water–manganite (γ-MnOOH) interface: II. An EXAFS study of zinc(II), J. Colloid Interface Sci. 229 (2000) 593–599.

[6] J.M. Boggs, M.A. Moscarello, in: P.C. Jost, O.H. Griffith (Eds.), Lipid–Protein Interactions, vol. 2, Wiley, New York, 1982.

[7] S. Brunauer, P.H. Emmett, E. Teller, Adsorption of gases in multimolecular layers, J. Am. Chem. Soc. 60 (1938) 309–319.

[8] P. Cavatorta, S. Giovanelli, A. Bobba, P. Riccio, A.G. Szabo, E. Quagliarello, Myelin basic protein interaction with zinc and phosphate: fluorescence studies on the water-soluble form of the protein, Biophys. J. 66 (1994) 1174–1179.

[9] P. D'Angelo, M. Benfatto, S. Della Longa, N.V. Pavel, Combined XANES and EXAFS analysis of Co^{2+}, Ni^{2+}, and Zn^{2+} aqueous solutions, Phys. Rev., B 66 (064209: 1/7).

[10] S. Della Longa, A. Arcovito, M. Girasole, J.L. Hazemann, M. Benfatto, Quantitative analysis of X-ray absorption near edge structure data by a full multiple scattering procedure: the Fe–CO geometry in photolyzed carbonmonoxy-myoglobin single crystal, Phys. Rev. Lett. 87 (15) (2001) 155501.

[11] S. Della Longa, A. Arcovito, M. Benfatto, A. Congiu-Castellano, M. Girasole, J.L. Hazemann, A. Lo Bosco, Redox-induced structural dynamics of Fe-Heme ligand in myoglobin by X-Ray absorption, Spectrosc. Biophys. J. 85 (2003) 549–558.

[12] C.E. Earl, A.C. Chantry, N. Mohammad, P. Glynn, Zinc ions stabilise the association of basic protein with brain myelin membranes, J. Neurochem. 51 (1988) 718–724.

[13] A. Filipponi, A. Di Cicco, C.R. Natoli, X-ray-absorption spectroscopy and n-body distribution functions in condensed matter: I. Theory, Phys. Rev., B 52 (21) (1995) 15122–15134.

[14] A. Filipponi, A. Di Cicco, C.R. Natoli, X-ray-absorption spectroscopy and n-body distribution functions in condensed matter: II. Data analysis and applications, Phys. Rev., B 52 (21) (1995) 15135–15149.

[15] R. Giovanoli, U. Leuenberger, Helv. Chim. Acta 52 (1969) 2333–2340.

[16] H. Haas, M. Torrielli, R. Steitz, P. Cavatorta, R. Sorbi, A. Fasano, P. Riccio, A. Gliozzi, Myelin model membranes on solid substrates. Thin Solid Films (1998) 327–329: 627–631.

[17] S.S. Hasnain, K.O. Hodgson, Structure of metal centres in proteins at subatomic resolution, J. Synchrotron Radiat. 6 (1999) 852–864.

[18] F. James, MINUIT, a package of programs to minimise a function of n variables, compute the covariance matrix, and find the true errors. Program library code D507, CERN (1978).

[19] Y. Joly, X-ray absorption near-edge structure calculations beyond the muffin-tin approximation, Phys. Rev., B 63 (125120-1/10).

[20] S. Kirkpatrick, C.D. Gelatt, M.P. Vecchi, Optimization by simulated annealing, Science 220 (1983) 671–680.

[21] S. Morante, The zinc environment in Langmuir–Blodgett phospholipid multi-layers, J. Synchrotron Radiat. 8 (2001) 975–977.

[22] J.E. Muller, O. Jepsen, J.W. Wilkins, X-ray absorption spectra: K-edges of 3d transition metals, L-edges of 3d and 4d metals and M edges of palladium, Solid State Commun. 42 (1982) 365–368.

[23] C.R. Natoli, in: A. Bianconi, L. Incoccia, S. Stipcich (Eds.), EXAFS and Near Edge Structure, Springer-Verlag, Berlin, 1983, p. 43.

[24] C.R. Natoli, M. Benfatto, A unifying scheme of interpretation of X-ray absorption spectra based on the multiple scattering theory, J. Phys. (France) Colloq. C8 47 (1986) 11–23.

[25] S. Nuzzo, C. Meneghini, S. Mobilio, H. Haas, P. Riccio, A. Fasano, P. Cavatorta, S. Morante, An X-ray absorption spectroscopy study of the zinc environment in Langmuir–Blodgett phospholipid multilayers, Biophys. J. 83 (2002) 3507–3512.

[26] J.J. Rehr, R.C. Albers, Theoretical approach to X-ray absorption fine structure, Rev. Mod. Phys. 72 (2000) 621–654.

[27] P.L. Riccio, L. Masotti, P. Cavatorta, A. De Sanctis, D. Juretic, A. Bobba, I. Pasquali-Ronchetti, E. Quagliarello, Myelin basic protein ability to organize lipid bilayers: structural transition in bilayers of lysophosphatidylcholine micelles, Biochem. Biophys. Res. Commun. 134 (1986) 313–319.

[28] T.A. Tyson, K.O. Hodgson, C.R. Natoli, M. Benfatto, General multiple scattering scheme for the computation and interpretation of X-ray absorption fine structure in atomic clusters with applications to SF_6, $GeCl_4$ and Br_2 molecules, Phys. Rev., B 46 (1992) 5997–6019.